

Interactions among physical and biological variables during the upwelling period in Monterey Bay, CA.

S. K. Service<sup>1</sup>, J. A. Rice<sup>2</sup> and F. P. Chavez<sup>1</sup>

<sup>1</sup>Monterey Bay Aquarium Research Institute

<sup>2</sup>Department of Statistics, University of California, Berkeley

## **Abstract**

We used data from moorings deployed in central California to examine the physical variables wind, PAR (photosynthetically available radiation) and temperature and the biological variable fluorescence during coastal upwelling. Variations of the multivariate techniques of principal components analysis and canonical correlation were used to extract the major modes of variability of these variables and to examine relationships among the variables. Data from both 1993 and 1994 indicate a consistent pattern of relationships among the physical variables, with NW winds and sunnier than average days leading lower than average temperatures at the mooring by 2-3 days. The relationship among the physical and biological variables was stronger in 1993 than in 1994. Higher than average fluorescence was found to lag lower than average temperatures, higher than average PAR and wind from the NW by 4, 6 and 7 days, respectively. The form of the relationship that produced maximal correlation between fluorescence and temperature was that several days of colder than average temperatures, followed by a trend to increased temperatures, was correlated with higher than average fluorescence. Higher than average fluorescence in 1993 showed maximal correlation with wind after several days of NW winds, followed by lighter winds from the SE. Relationships among physical variables and fluorescence are not as strong in 1994 as in 1993, and we hypothesize these differences to be related to differences in the strength and duration of upwelling in the two years.

## Introduction

Satellite images of sea surface temperature (SST) of the ocean off central and northern California show a continuous band of cool water next to the coast after several days of northwesterly winds during the spring. This cool water is the product of coastal upwelling, a process that drives deeper, colder, nutrient-rich water to the surface (see Barber and Smith (1981) and references therein for a detailed description of the coastal upwelling process and its biological and chemical consequences). These cool, nutrient-rich waters can support extensive phytoplankton populations (or blooms) that eventually lead to large clupeid fisheries (Ryther, 1969; Barber and Chavez, 1983; Bakun, 1996). A closer look at the SST images reveals that the coldest waters are often centered around specific coastal features, such as capes or points (Strub *et al.*, 1991). For example, in Monterey Bay, the coldest water is often observed north of the Bay (Rosenfeld *et al.*, 1994, Figure 1). These colder upwelling “centers” may be the source of the upwelled water found further downstream, although it is likely that coastal upwelling occurs along the entire northern and central California coast. Freshly upwelled water is low in phytoplankton biomass; additionally these upwelled phytoplankton populations may not be fully acclimated to their environment, resulting in a time lag between the introduction of the upwelled water to the surface and subsequent phytoplankton blooms. While the development of springtime phytoplankton blooms has been previously documented for Monterey Bay (Bolin and Abbott, 1963; Malone, 1971; Chavez, 1995 1996), a systematic study of upwelling events and phytoplankton blooms has yet to be completed. The lag between events in the upwelling cycle in Monterey Bay, from initiation of upwelling north of the Bay to the appearance of phytoplankton blooms in the Bay, has only recently been examined (Sakamoto *et al.*, 1997; Kudela *et al.*, 1997) and has not been documented under a variety of conditions or on the appropriate time scales.

Since 1992, the Monterey Bay Aquarium Research Institute (MBARI) has maintained two moorings in and offshore of the Bay that regularly measure a number of meteorological, physical, chemical and biological variables (Chavez *et al.*, 1997). Data from these moorings provide an ideal setting to continuously examine upwelling throughout a season, rather than relying on discrete shipboard measurements. Records over an entire season encompass many types of upwelling events, and enable ready assessment of time-varying and co-varying aspects of measured variables under different conditions. In this contribution we use physical and biological data collected on the moorings during the upwelling seasons of 1993 and 1994 to (1) describe the major modes of variability of these variables, (2) assess their time-varying patterns, (3) examine their relationships, and (4) describe the average timing of events for an upwelling cycle in Monterey Bay. To accomplish these four aims we used two complementary analysis techniques. One is a method based on Principal Component Analysis (PCA). The second method is new to the field of oceanography and is a penalized form of Canonical Correlation (PCC). Modifications of these classical multivariate techniques for the analysis of random curves, or profiles, has come

to be known as “functional data analysis” (Ramsey and Silverman, in press). Part of our interest was in ascertaining how well these techniques could be employed in a time series setting to extract important information concerning the short-term (days) nature of climatic (wind) and biological (phytoplankton) coupling in a coastal upwelling system.

## Data and Methods

### Data

We used measurements of sea-surface temperature, fluorescence and photosynthetically available radiation (PAR) from MBARI’s M1 mooring in the mouth of Monterey Bay (Figure 1, 36.7°N, 122.0°W). PAR is a measure of light in the range important for photosynthesis, and fluorescence is an estimate of phytoplankton biomass (Kirk, 1994). The moorings themselves, and the various sensors deployed on them, are described in detail in Chavez *et al.* (1997). We used wind data from MBARI’s offshore M2 mooring (Figure 1, 36.7°N, 122.4°W) so that the wind field would be less affected by heating and cooling of land and therefore more representative of oceanic conditions. Wind data were in vector form, with one component representing wind strength in the east-west direction ( $u$ ) and one component representing wind strength in the north-south direction ( $v$ ). Each of these variables was measured every 10 minutes, making 144 measures for a 24 hour period.

Since the upwelling season in Monterey Bay typically begins in spring and lasts through summer, we used data from Julian Days 61 - 244 (March through August) collected in 1993 and 1994. While the sensors measure data every 10 minutes, there are gaps in the record due to sensor or system malfunction, maintenance and calibration. Our method of analysis required that a complete day’s record (144 measurements) be available for each of the 4 variables in order for data for that day to be used in the analysis. When preparing the data, if gaps in the record for any variable existed that were less than 2 hours long, the gap was filled by linear interpolation. If gaps of more than 2 hours existed for a given day for any of the four variables (either in one gap or in several smaller gaps), that day was considered missing. After filling gaps less than 2 hours, there were 178 days of data with a complete record for temperature, fluorescence, PAR and wind in 1993, and 173 such days of data for 1994. The data from 1993 were used to develop hypotheses and predictions, which were then examined with the 1994 data.

### Methods

Annual trends were first removed from each variable by fitting a constant, a cosinusoid of period one year, and a cosinusoid of period one-half year by least squares and then subtracting the result from the original data. All subsequent analyses were performed on these residual series.

Principle components analysis (PCA) was used to extract the major modes of daily variability from each of the series. In standard PCA, the vector of length  $p$  of one day's temperature profile,  $X_t$ , for example is decomposed into the sum of a vector  $m$ , which is the componentwise mean of  $T$  daily measurements, and scalar multiples  $\Lambda_{kt}$  of eigenfunctions  $V_k$  of length  $p$ :

$$X_t = m + \sum_{k=1}^p \Lambda_{kt} V_k.$$

The eigenfunctions  $V_k$  are the eigenvectors of the covariance matrix of the collection of  $T$  daily temperature profiles. That day's score,  $\Lambda_{kt}$ , on the  $k^{\text{th}}$  eigenvector is the dot product of  $X_t$  and  $V_k$ . The eigenvector  $V_k$  has associated eigenvalue

$$\lambda_k = \frac{1}{T} \sum_{t=1}^T \Lambda_{kt}^2.$$

In our application of PCA,  $p=144$ , and  $T=178$  in 1993 and 173 in 1994. In the case of the wind variable, PCA was accomplished by stacking each day's  $u$  and  $v$  measurements to form a vector of length  $2p$ . We employed a slight modification of this procedure in which the eigenfunctions were approximated by cubic spline functions with breakpoints every two hours. This reduced the size of the calculations and also produced smoother eigenfunctions. As will be demonstrated in the next section, the first few eigenfunctions account for a large proportion of the total variability and represent smooth anomalies, or deviations from the mean. The higher order eigenfunctions become increasingly oscillatory and account for less of the variability. PCA has been used extensively in physical oceanography, often under the name of empirical orthogonal functions. It has been applied to a phytoplankton series by Cloern and Jassby (1995).

As well as examining cross-correlation functions of scores on the eigenfunctions, we used a modified form of canonical correlation analysis to search more specifically for relationships among major modes of variability. In standard canonical correlation analysis (Mardia *et al.* 1979) one finds vectors  $a$  and  $b$  to maximize  $(a^T S_{XY} b)^2$  subject to  $a^T S_{XX} a = b^T S_{YY} b = 1$  where the matrices  $S$  are covariance and cross-covariance matrices as indicated by their subscripts. In contexts such as ours in which the vectors are quite large, since the results are dominated by noise, smoothing is essential to obtain meaningful results. Leurgans, Moyeed, and Silverman (1993) proposed modifying the constraints by adding a roughness penalty. In particular, they investigated maximizing  $(a^T S_{XY} b)^2$  subject to the constraints

$$\begin{aligned} a^T S_{XX} a + \omega a^T D^4 a &= 1 \\ b^T S_{YY} b + \omega b^T D^4 b &= 1 \end{aligned}$$

where  $D^4$  is a discretized version of a fourth derivative operator. This procedure penalizes solutions that have large second derivatives and thus pulls solutions toward smooth low degree polynomials. As  $\omega \rightarrow \infty$ , the solutions of the penalized problem tend to linear functions.

We modified this procedure by replacing the roughness measure  $a^T D^4 a$  by  $a^T S_{XX}^{-1} a$ , for example. This measure can be expressed in terms of the eigenvectors and eigenvalues of  $S_{XX}$  as

$$a^T S_{XX}^{-1} a = \sum_{k=1}^n \frac{(a^T V_k)^2}{\lambda_k}$$

and using it as a penalty thus pulls the solutions toward the eigenfunctions with large eigenvalues, that is towards smooth major modes of variability.

In the simplest application of this methodology, the canonical vectors, or functionals,  $a$  and  $b$  correspond to deviations from the mean daily profiles of variables such as temperature and fluorescence, for example, and our penalized canonical correlation analysis (PCC) is an attempt to find which such anomalies are strongly related to each other. It is partly because of this interpretation that a penalty that pulls solutions towards linear functions is not entirely appropriate, since PAR anomalies, for example, do not look like low degree polynomials because PAR is zero during the evening hours.

More generally,  $a$  and  $b$  need not be of the same length, and in the next section we will allow  $a$ , for example, to represent a temperature anomaly over a several day period and  $b$  a fluorescence anomaly only over the last day of that period. This allows us to look for lagged relationships among the variables. As in the case of PCA, the score of a given profile is its dot product with the corresponding canonical vector.

Here also we have found it computationally convenient to approximate the canonical functionals by cubic splines, again using breakpoints every two hours. Doing so also resulted in smoother curves. Also, in order for the same penalty parameter  $\omega$  to be used for both roughness measures we scaled the data so that the traces of both covariance matrices were equal to one.

We chose to use large values of  $\omega$ , so that we were effectively maximizing  $(a^T S_{XY} b)^2$  subject to  $a^T S_{XX}^{-1} a = b^T S_{YY}^{-1} b = 1$ . Cross validation, as described in Leurgans *et al.* (1993) would have been another possibility. The effects of these and other subjective choices made during the analysis were controlled in the following way. We first conducted extensive analysis of the 1993 series before examining the 1994 series in any way. On the basis of the 1993 analysis we formulated a number of explicit predictions for the 1994 series, regarding the major modes of variability of the different variables and the nature and timing of relationships among variables. These predictions were then tested on the 1994 data.

## Results and Discussion

### The Raw Data

Plots of the daily means of temperature, fluorescence, PAR and wind for 1993 and 1994 show predominate features of the upwelling season: (1) low surface temperatures, (2) phytoplankton blooms, (3) seasonal increase in solar irradiance and (4) NW winds (Figures 1-4). Daily means are plotted in Figures 2-3 for simplicity, a full day's profile was used in analyses. To illustrate the typical daily profiles of the four variables examined Julian day 155 in 1994 was plotted separately (Figure 4). Julian day 155 was mostly sunny, with light winds offshore during morning and evening, and onshore during mid-day. The sunny mid-day conditions resulted in warming of surface waters of over one degree Celsius, with the light winds likely contributing to the magnitude of this surface warming. Fluorescence shows the typical mid-day decrease coincident with high light conditions. This diurnal variability in fluorescence is due to non-photochemical quenching during daylight (Kiefer, 1973).

### **Major modes of variability of temperature, fluorescence, PAR and wind**

The first three eigenfunctions accounted for 98.5% of the total variability in temperature, 92.3% of the variability in fluorescence, 95.2% of the variability in PAR and 91.6% of the variability in wind in 1993. The forms of the first three eigenfunctions for the three scalar variables temperature, fluorescence and PAR were remarkably similar (Figure 5). In all of these plots, magnitude of the eigenfunction is on the y axis and time of day is on the x axis, with each eigenfunction being of dimension 1 by 144 (one weight given to each measurement through the day). Weights for the first eigenfunction for temperature and fluorescence were positive for all 144 times during the day and the range of magnitude of the weights is very small. The first eigenfunction of PAR also has all positive weights, with the middle of the day most heavily weighted. For all three variables, a deviation proportional to the first eigenfunction (and therefore the primary mode of variability) amounts to a shift in overall level. In the case of PAR, of course, this shift only occurs during the daylight hours, and there is some slight deviation from uniformity in the other variables as well. A positive deviation of temperature in the direction of the first eigenfunction would amount to slightly more warming during the late afternoon hours than during the morning hours.

The second most important mode of variability for both temperature and fluorescence is represented by an increasing trend through the day (Figure 5). Since weights on the second eigenfunction are negative in the first half of the day, and positive in the second half, a positive deviation from the mean in the direction of the second eigenfunction would amount to decreased magnitude in the morning hours and increased magnitude during the later hours. For PAR this second mode of variability is represented by a peak shift, with peak sunlight shifted to earlier in the day, and the afternoon receiving negative weights. This is essentially a decreasing trend in PAR through the day.

The third most important mode of variability for temperature and fluorescence shifts the dynamics of a daily profile by decreasing the value of the variable at mid-day and increasing it in the early and late hours (Figure 5). Because a typical daily profile of temperature shows some mid-day warming of surface waters (Figure 4), this eigenfunction serves to flatten the daily profile of temperature. The typical daily profile of fluorescence, however, has a decrease at mid-day (Figure 4). This eigenfunction, then, serves to accentuate this mid-day decrease. The third eigenfunction for PAR is similar, in that it sharpens the mid-day peak of PAR.

Wind is a vector-valued variable, and therefore its eigenfunctions are of dimension 2 by 144. The corresponding  $u$  and  $v$  components can also be represented as magnitude and direction. The major mode of variability in wind is represented by winds of constant magnitude from the NW (Figure 5). The second most important mode of variability in wind is represented by a shift in wind direction from the SE before noon to the NW after noon. The third most important source of variability is represented by the classical daily pattern of coastal wind fields, the wind being offshore in the morning and late afternoon/evening, and onshore during the middle of the day (Figure 4).

We predicted that the eigenfunctions from the 1994 data would be similar to the 1993 data, and indeed they are nearly identical (data not shown). In 1994, the first three eigenfunctions accounted for 92.5% of the variability in fluorescence, 95.7% of the variability in PAR, 96.8% of the variability in temperature and 88.9% of the variability in wind. These modes of variability, then, appear to be regular features during the upwelling period.

In order to examine how the major modes of variability of each of these variables changes through time, we calculated, for each day analyzed, the score for a given variable on a particular eigenfunction. These scores can then be viewed as a time series, and autocorrelations calculated. Autocorrelations of the first eigenfunctions of temperature, fluorescence and wind remained positive and above 0.20 for up to two days in 1993 (autocorrelations at lag 2: temperature  $r=0.71$ , fluorescence  $r=0.42$ , wind  $r=0.30$ ), whereas autocorrelations for the first eigenfunction of PAR were 0.08 at two days. These patterns were true for 1994 as well (autocorrelations at lag 2: temperature 0.63, fluorescence 0.56, PAR 0.16, wind 0.21). As the first eigenfunction represents overall level of a given variable, this autocorrelation indicates, for example, that if fluorescence is higher than average it can be expected to remain relatively so for several days. The autocorrelation of temperature was the longest of any of the variables examined. The autocorrelation of temperature was above zero for up to 10 days in 1993 and 12 days in 1994. In 1993 the autocorrelation of fluorescence was equal to zero after 3 days, however in 1994 this decorrelation scale was much longer (14 days). These decorrelation scales in 1994 are longer than that found by Abbott and Letelier (1997), using instrumented drifters. The second mode of variability fluctuates more rapidly than the first, and this is borne out in the autocorrelation func-

tions (not shown); the autocorrelations of the second eigenfunctions dropped quickly to zero, and oscillated around this level with few identifiable peaks.

Cross-correlations between these scores measure the relationships among the major modes of variability of each of the variables. These relationships are examined in the next section, along with the results of the PCC analysis.

## **Relationships among temperature, fluorescence, PAR and wind**

We examined the cross-correlations between the scores from the PCA analysis among all variables. Since there were four variables (temperature, fluorescence, PAR and wind) and 3 eigenfunctions per variable, this resulted in 66 cross-correlation functions. Only the lag window of -10 to 10 days was examined. We examined only the highest-order eigenfunctions in the PCC analysis, and the output from this analysis includes not only the eigenfunctions that describe the relationship, but a series of scores for each of the two variables that indicate the strength of the relationship on a particular day. As both analyses measure relationships between pairs of variables, results from both analyses are presented below for each pairwise comparison.

### *Wind & PAR*

The maximum correlation between the first eigenfunction of wind and the first eigenfunction of PAR was at 0 lag in both 1993 and 1994 (1993  $r=0.49$ , 1994  $r=0.55$ ). The form of the relationship is that strong winds from the NW produce sunnier than average days. The eigenfunctions from the PCC analysis show the same relationship in both 1993 and 1994 (Figure 6), with correlations of a similar magnitude (1993  $r=0.51$ , 1994  $r=0.52$ ). Time series plots of the scores from the PCC analyses show that the scores track one another fairly well (Figure 7). The corresponding plot of PCA scores is very similar (data not shown). This general relationship holds when looking at other modes of variability identified in the PCA analysis. For example, the maximum correlation between the second eigenfunction of wind and the first eigenfunction of PAR was at a lag of 1 day (1993  $r=0.21$ , 1994  $r=0.22$ ). In both years the form of the relationship was the same: the day after winds switch from SE to NW, the weather is sunnier than average. Upwelling-favorable winds tend to be associated with sunny weather. The relationships predicted from the 1993 data were upheld with the 1994 data.

### *Wind & Temperature*

The first eigenfunction of temperature and the first eigenfunction of wind were maximally correlated at a lag of 2 days in 1993 ( $r=-0.52$ ) and 3 days in 1994 ( $r=-0.46$ ). The negative sign of the correlation indicates that NW winds are associated with lower than average temperatures 2-3 days later. Again, the form of the eigenfunctions from the PCC analysis show similar results for both 1993 and 1994 (Figure 8). Because we were interested in

wind events preceding temperature events, we used in the PCC analysis the correlation between a given day of temperature and three days (that same day and two days previous) of wind. The PCC analysis defines the nature of the relationship more precisely than does the PCA analysis, in that three days of strong winds from the NW is associated with lower than average temperatures (Figure 8). The correlations from the PCC analysis were 0.58 for 1993, and 0.43 for 1994, and the time series plots of scores on the PCC analyses follow each other well (Figure 9) except for most notably during the period Julian Day 130-160 of 1994. During this period, winds were from a NW direction, however three days later temperatures remained higher than average.

Examining the cross-correlations between other modes of variability identified in the PCA analysis confirms the tight coupling between these variables. The maximum correlation between the first eigenfunction of wind and the second eigenfunction of temperature was at 0 lag in both 1993 and 1994 (1993  $r=-0.46$ , 1994  $r=-0.28$ ), indicating that if the wind was blowing from the NW the surface temperatures at M1 were declining. In fact, temperatures at M1 have a decreasing trend on days that the wind switches from SE to NW (1993  $r=-0.24$ , 1994  $r=0.17$ ). Predictions from the 1993 analyses were consistent with 1994 results. In both years, the relationships between the first eigenfunctions of wind and temperature would seem to indicate that it takes approximately 2-3 days for water that is newly upwelled north of the Bay to reach the M1 buoy in the mouth of the Bay. This is in agreement with previous drifter studies conducted in Monterey Bay (Chavez *et al.* 1997).

### *PAR & Temperature*

The results from the PCC analysis demonstrate that lower than average temperatures are associated with having increasingly sunny weather in preceding days (Figure 10). The correlation between temperature and PAR on that day and 2 days previous (the relationship pictured in Figure 10) was 0.25 in 1993 and 0.33 in 1994. The correlations increase, however, the further back in time that one examines PAR, up to  $r=0.50$  in 1994 for the correlation between temperature and PAR on that day and 7 days previous.

In 1993 the maximum correlation between the first eigenfunctions of PAR and temperature was with temperature lagging PAR 2 days ( $r=-0.21$ ). The correlation for this lag in 1994 was  $-0.27$ , however the correlation increased to  $-0.34$  for a 9-day lag. The precise timing of the maximum correlation from the PCA analysis in 1994, then, was not well predicted by the analysis of the 1993 data. A correlation between PAR and temperature at a lag of 2-3 days would match well with the correlation between wind and PAR (0-lag) and between wind and temperature (2-3 day lag).

The PCA analysis also demonstrated that the maximal correlation between the third eigenfunction of temperature and the first eigenfunction of PAR were maximally correlated at a lag of 0 days. The third eigenfunction of temperature represents a flattening of the daily

profile of temperature. As the correlation was negative (1993  $r=-0.35$ , 1994  $r=-0.32$ ) this amounts to the intuitive result that sunnier than average days result in mid-day warming of surface waters. While this may seem in contradiction to results stated previously (with sunnier than average days associated with colder than average overall temperatures), remember that the eigenfunctions are uncorrelated with one another and each of these functions is highlighting a unique mode of variability in temperature.

### *Physical Variables & Fluorescence*

While correlations among the physical variables were relatively large and consistent from year to year, relationships involving the biological variable (fluorescence) were less strong. In general, correlations involving fluorescence were higher in 1993 than in 1994. In 1993 fluorescence was most strongly correlated with temperature. The maximum correlation between the first eigenfunctions of fluorescence and temperature was when fluorescence lagged temperature by four days ( $r=-0.3929$ ). The negative sign of the correlation indicates the inverse relationship between these two variables, with lower than average temperatures being associated with higher than average levels of fluorescence four days later.

The PCC analysis refined the relationship between temperature and fluorescence somewhat, in that four days of lower than average temperatures, followed by a day with a trend to increasing temperatures, were associated with higher than average levels of fluorescence (Figure 11). The corresponding correlation was 0.40.

The results for 1994 have similar relationships and timing (data not shown), however the correlations decrease. The correlation from the PCA result was only -0.12, (at a lag of three days) and that from the PCC analysis was also 0.12 (with three days of colder than average temperatures, followed by a warming trend associated with higher than average levels of fluorescence).

Given that wind is maximally correlated with temperature at about a two day lag (as is PAR), and temperature maximally correlated with fluorescence at approximately a four day lag, one would expect the strongest relationships between wind and fluorescence (or PAR and fluorescence) to be at about a six day lag. In 1993 the maximum correlation between the first eigenfunction of wind and the first eigenfunction of fluorescence was 0.35 at a lag of seven days, and in 1994 this maximum correlation was 0.11 at six days. In both years the form of the relationship was the same - winds from the NW produce higher than average levels of fluorescence 6-7 days later. When examining the relationship between the first eigenfunctions of PAR and fluorescence, the maximum correlation in 1993 was 0.23 at a lag of 6 days, in 1994 the maximum correlation was 0.18 at a lag of seven days. The form of the relationship was the same in both years with sunnier than average days being followed 6-7 days later by higher than average fluorescence levels.

The relationship between wind and fluorescence is made more clear using the PCC analysis, with data from 1993 presented as an example (Figure 11). Notice the close similarity of the fluorescence anomalies most closely related to temperature and wind and that both are essentially the first eigenfunction from the PCA analysis on fluorescence. When examining fluorescence and wind on that day and 5 days previous, one sees that higher than average levels of fluorescence are associated with several days of strong winds from the NW followed by lighter winds from the SE (Figure 11), however this pattern is not as clear when examining 1994 results (data not shown). Light or SE winds, following upwelling favorable winds, are thought to be necessary before phytoplankton blooms are observed at the M1 mooring site.

Correlations with the third eigenfunction of fluorescence, indicating the strength of the diurnal signal, were high only with the first eigenfunction of PAR (1993  $r=0.25$ , 1994  $r=0.18$ ). The strength of the fluorescence diurnal signal did not appear to be related to temperature or wind. Stramska and Dickey (1992a) also found short-term variations in fluorescence to be primarily related to PAR and found little correlation between the diurnal cycle of fluorescence and temperature (1992b).

## Conclusions and Summary

Analysis of data collected in 1993 from moorings in central California indicate a consistent pattern of relationships among physical and biological variables during the upwelling period. As winds in the Bay area change from SE to NW, skies begin clearing. The following day, the wind is strong out of the NW, and skies remain clear. Surface water temperatures begin to decline, initiating Day 1 of upwelling. By Day 3 the coldest water associated with the upwelling event has reached M1, and by Day 7 the fluorescence signal from the phytoplankton has reached a peak. This fluorescence peak was associated with several days of NW winds, followed by winds from the SE. Work in other upwelling systems in California has also indicated a lag of approximately 6-10 days between initiation of upwelling and peak phytoplankton blooms (Dugdale and Wilkerson, 1989). Analysis of 1994 data indicated the same, consistent pattern among the physical variables; however the relationship between these variables and fluorescence were much weaker.

What could be responsible for the year-to-year changes in the strengths of the relationships between physical and biological variables? The answer to this question may lie in an analysis of phytoplankton growth in upwelling systems. Upwelling centers are analogous to a chemostat (Chavez, 1995), in that the freshly upwelled water acts as a continuous “inflow” of fresh nutrients to the phytoplankton populations. The NW upwelling winds advect the “outflow” of this chemostat downstream of the main upwelling center (Rosenfeld *et al.*, 1994). During periods of intense upwelling, if the rate of inflow is greater than the phytoplankton growth rate, the phytoplankton populations will not increase at upwelling centers, while populations downstream (“outflow” areas) will increase. Strong, sustained, upwelling increases the area affected by this outflow, and peak phytoplankton populations will be located further from the upwelling centers. Wind reversals change the advective patterns (Rosenfeld *et al.*, 1994) and result in the advection of these downstream phytoplankton populations back over the site of active upwelling. The fluorescence record at the M1 mooring (located close to an upwelling center) is then a function not only upwelling itself but also of the frequency and duration of wind reversals.

If we examine temperature and wind data from the M1 and M2 moorings we find 1994 to be, on average, a colder year than 1993, with stronger NW winds. The average surface water temperature at M1 during the upwelling period in 1993 was 13.15°C, while in 1994 it was 12.11°C. In 1993, 25% of the days during the upwelling period had mean daily surface water temperatures less than 12°C, whereas 46% of 1994 mean daily temperatures were less than this level. Winds during the upwelling period averaged 6.5 meters·sec<sup>-1</sup> in 1994 and 6.0 meters·sec<sup>-1</sup> in 1993, and the percentage of days during the upwelling period during which the daily mean wind speed was greater than 6.0 meters·sec<sup>-1</sup> was 49% in 1993 and 59% in 1994. The increased strength of upwelling in 1994 pro-

longed the time the M1 mooring measured freshly upwelled waters. This effect can be seen in the plots of daily means, where during Julian days 150-200 in 1994 (Figure 3), fluorescence shows a decrease, coincident with strong NW winds, few wind reversals and low surface temperatures. After Julian day 200 there is a cessation of NW upwelling winds, and the southerly winds bring water with higher phytoplankton concentrations past M1. The longer autocorrelation scales seen for temperature and fluorescence in 1994, as compared to 1993, support the hypothesis that the M1 mooring measured freshly upwelled waters for a longer period of time in 1994.

The use of PCA enabled dissection of the physical and biological time series into orthogonal components with interpretable meaning, and the PCC analysis resulted in detection of subtle aspects of relationships among the measured variables. For example, PCA revealed the maximum correlation between upwelling-favorable winds and high phytoplankton biomass (as measured by fluorescence) to be at a lag of six to seven days; however the PCC analysis from 1993 showed the actual form of this relationship to be several days of strong NW winds followed by lighter SE winds. The PCC results, then, emphasize the importance of wind reversals to the detection of phytoplankton blooms at M1.

The comparison between 1993 and 1994 data illustrate that understanding the relationship through time between physical and biological variables measured at a mooring requires more than a cursory understanding of the spatial patterns associated with upwelling. Teasing apart the influences of local vs advective effects can be difficult for data measured on moored systems (see for example Dickey *et al.*, 1991; 1993). In contrast, when the same water mass is followed (as with a drifter) a more straightforward interpretation of such relationships through time may be developed; however drifters provide far less data, over a much shorter time scale, than do moorings. Additionally, interpretation of drifter data also requires careful analysis (Abbott *et al.*, 1995). The inference from moored data systems can be increased through additional systems deployed at strategic locations in the upwelling space-time continuum, and by integration with data measured from ships and satellites (Dickey *et al.*, 1993). In upwelling systems with a well-established spatial pattern, as in central California, additional moorings downstream from an upwelling center may provide the spatial and temporal coverage necessary to better understand the relationship between physical and biological variables.

#### Acknowledgments

JR thanks the National Security Agency for funding and Richard Olshen for stimulating conversations. Reiko Michisaki made the most excellent Figure 1. Thanks to Raphael Kudela for discussions about bio-optics, JT Pennington for mooring maintenance and the David and Lucile Packard Foundation for financial support to FPC.

## References

- Abbott, M. R., K. H. Brink, C. R. Booth, D. Blasco, M. S. Swenson, C. O. Davis and L. A. Codispoti (1995) Scales of variability of bio-optical properties as observed from near-surface drifters. *J. Geophys Res* 100:13345-13367.
- Abbott, M. R. and R. M. Letelier (1997) Bio-optical drifters - scales of variability of chlorophyll and fluorescence. In: *Ocean Optics XIII*, S. G. Ackleson, R. Frouin, Proc. SPIE 2963:216-221.
- Bakun, A (1996) *Patterns in the Ocean: Ocean processes and marine population dynamics* California Sea Grant College System and the National Oceanic and Atmospheric Administration.
- Barber, R. T. and R. L. Smith (1981) Coastal upwelling ecosystem. In: *Analysis of marine ecosystems*, A. Longhurst. Academic, pp 31-68.
- Barber, R. T. and F. P. Chavez (1983) Biological consequences of El Niño. *Science* 222:1203-1210.
- Bolin, R. L., and D. P. Abbott. (1963) Studies on the marine climate and phytoplankton of the central coastal area of California, 1954-1960. *Calif. Coop. Oceanic Fish. Invest. Rpt.* 9: 23-45.
- Chavez, F. P. (1995) A comparison of ship and satellite chlorophyll from California and Peru. *J. Geophys. Res.* 100: 24855-24862.
- Chavez, F. P. (1996) Forcing and biological impact of onset of the 1992 El Niño in central California. *Geophys. Res. Letters.* 23: 265-268.
- Chavez, F. P., J. T. Pennington, R. Herlien, H. Jannasch, G. Thurmond and G. E. Friedrich. (1997) Moorings and drifters for real-time interdisciplinary oceanography. *J. Atmos. Oceanic Tech.* In press.
- Cloern, J.E. and A.D. Jassby (1995). Year-to-Year fluctuation of the Spring phytoplankton bloom in South San Francisco Bay: an example of ecological variability at the land-sea interface. In: *Ecological Time Series*, T.M. Powell and J.H. Steele. Chapman and Hall.
- Dickey, T., J. Marra, T. Granata, C. Langdon, M. Hamilton, J. Wiggert, D. Siegel and A. Bratkovich (1991) Concurrent high resolution bio-optical and physical time series observations in the Sargasso Sea during the spring of 1987. *J. Geophys. Res.* 96:8643-8663
- Dickey, T., T. Granata, J. Marra, C. Langdon, J. Wiggert, Z. Chai-Jochner, M. Hamilton, J. Vazquez, M. Stramska, R. Bidigare and D. Siegel (1993) Seasonal variability of bio-optical and physical properties in the Sargasso Sea *J. Geophys. Res.* 98:865-898
- Dugdale, R. C. and F. P. Wilkerson (1989) New production in the upwelling center at Point Conception, California: temporal and spatial patterns. *Deep Sea Res.* 36:985-1007.
- Kiefer, D. A. (1973) Fluorescence properties of natural phytoplankton populations. *Mar. Biol.* 22:263-269.
- Kirk, J. T. O. (1994) *Light and photosynthesis in aquatic ecosystems*. Cambridge

- Kudela, R. M., W. P. Cochlan and R. C. Dugdale. (1997) Carbon and nitrogen uptake response to light by phytoplankton during an upwelling event. *J. Plankton Res.* In press.
- Leurgans, S.E., R.A. Moyeed, and B.W. Silverman (1993). Canonical correlation when the data are curves. *J. R. Statist. Soc. B*, **55**, 725-740.
- Malone, T. C. (1971) The relative importance of nannoplankton and netplankton as primary producers in the California Current system. *Fish. Bull.* 69: 799-820.
- Mardia, K. V., Kent, J. T. and J. M. Bibby (1979) *Multivariate Analysis*. Academic Press.
- Ramsay, J. O. and B. W. Silverman (1997) *Functional Data Analysis* In press.
- Rosenfeld, L., F. Schwing, N. Garfield, and D. E. Tracy (1994) Bifurcated flow from an upwelling center: a cold water source for Monterey Bay. *Cont. Shelf Res.* 14: 931-964.
- Ryther, J. H. (1969) Photosynthesis and fish production in the sea. *Science* 166:72-76.
- Sakamoto, C. M., Friederich, G. E., S. K. Service and F. P. Chavez (1996). Development of automated surface seawater nitrate mapping systems for use in open ocean and coastal waters. *Deep-Sea Res.* 43:1763-1775.
- Stramska, M. and T. D. Dickey (1992a) Short-term variations of the bio-optical properties of the ocean in response to cloud-induced irradiance fluctuations. *J. Geophys. Res.* 97:5713-5721
- Stramska, M. and T. D. Dickey (1992b) Variability of bio-optical properties of the upper ocean associated with diel cycles in phytoplankton population. *J. Geophys. Res.* 97:17873-17887
- Strub, P. T., P. M. Kosro and A. Huyer (1991) The nature of cold filaments in the California Current System. *J. Geophys. Res.* 96:14743-14768.

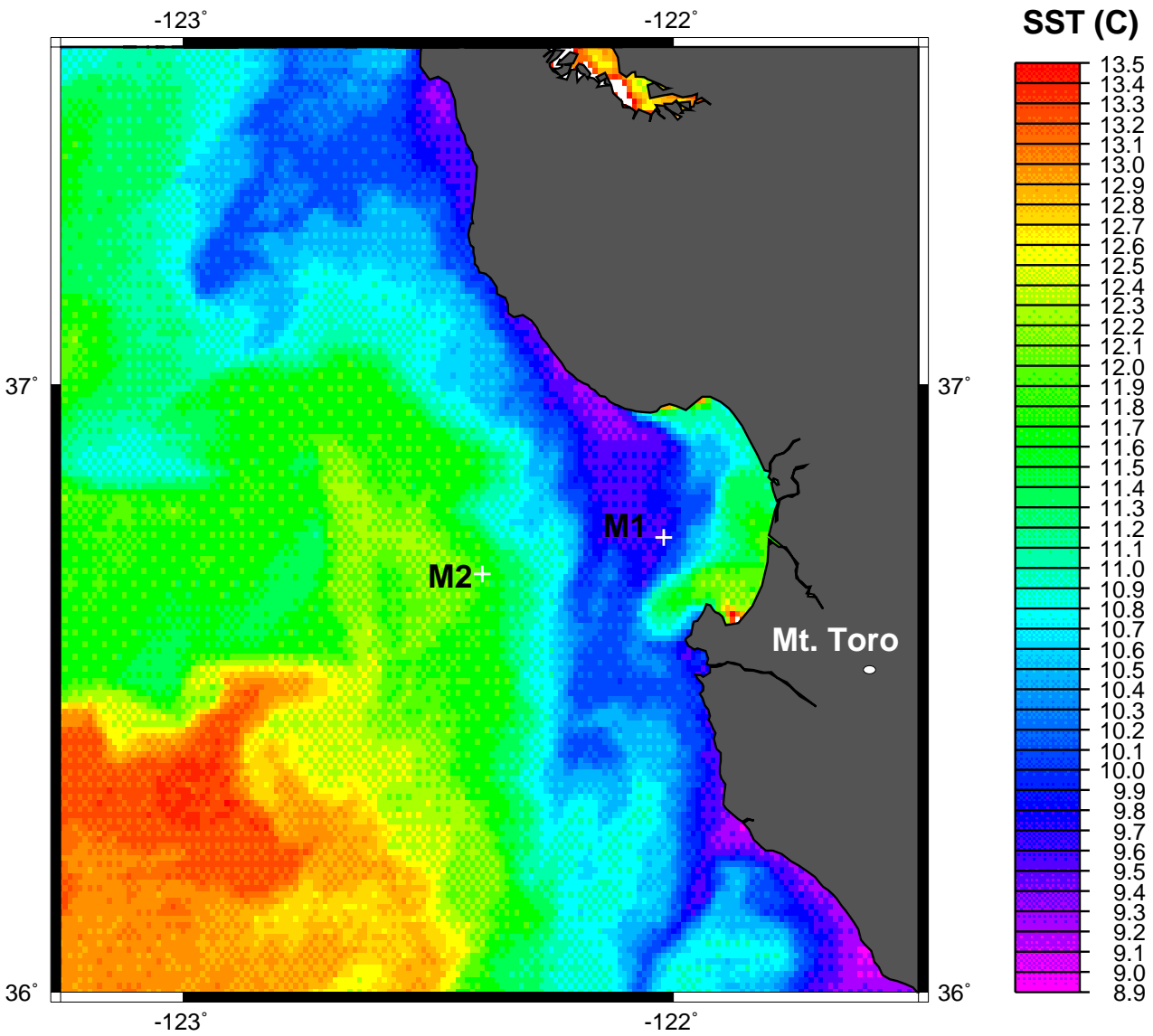


Figure 1. A VHR image from April 21, 1995, indicating sea surface temperature in Monterey during an upwelling event. The locations of the M1 and M2 moorings are shown.

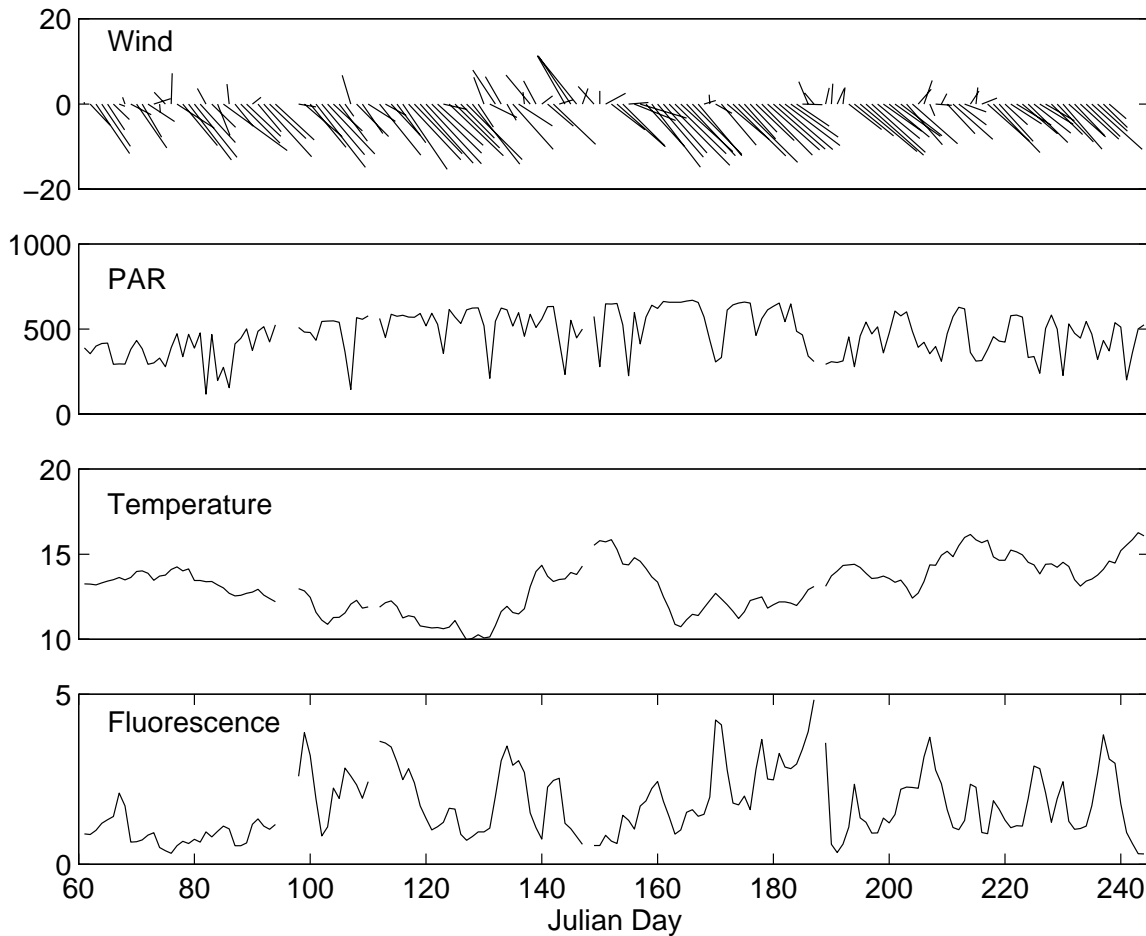


Figure 2. Plots of daily mean wind, PAR, temperature and fluorescence for 1993. Gaps in the time series are indicated by blanks. Units for wind, PAR, temperature and fluorescence are meters  $\text{sec}^{-1}$ , microEinstens  $\text{meter}^{-2} \text{sec}^{-1}$ , degrees Celsius and volts, respectively.

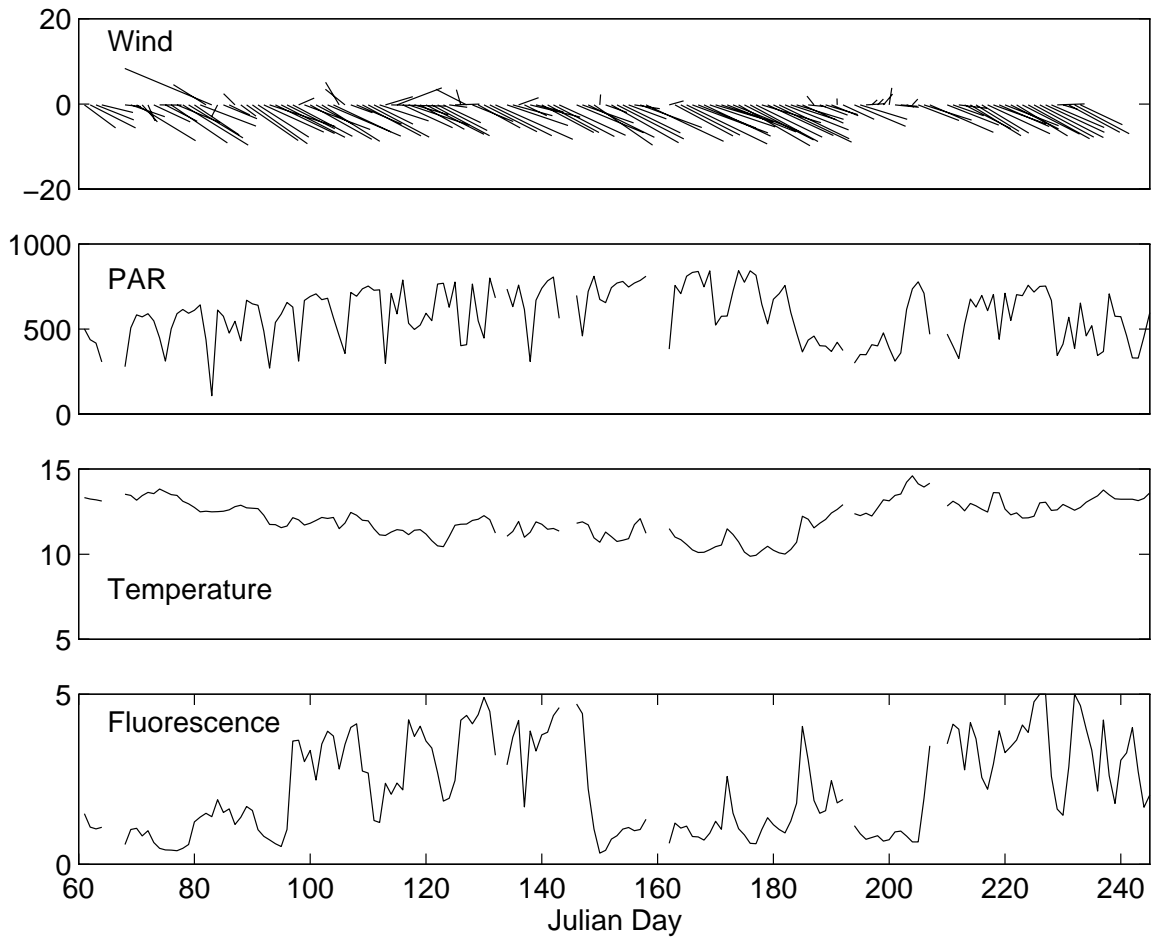


Figure 3. Plots of daily mean wind, PAR, temperature and fluorescence 1994. Gaps in the time series are indicated by blanks. Units for wind, PAR, temperature and fluorescence are  $\text{meters}\cdot\text{sec}^{-1}$ ,  $\text{microEinstens}\cdot\text{meter}^{-2}\cdot\text{sec}^{-1}$ , degrees Celsius and volts, respectively.

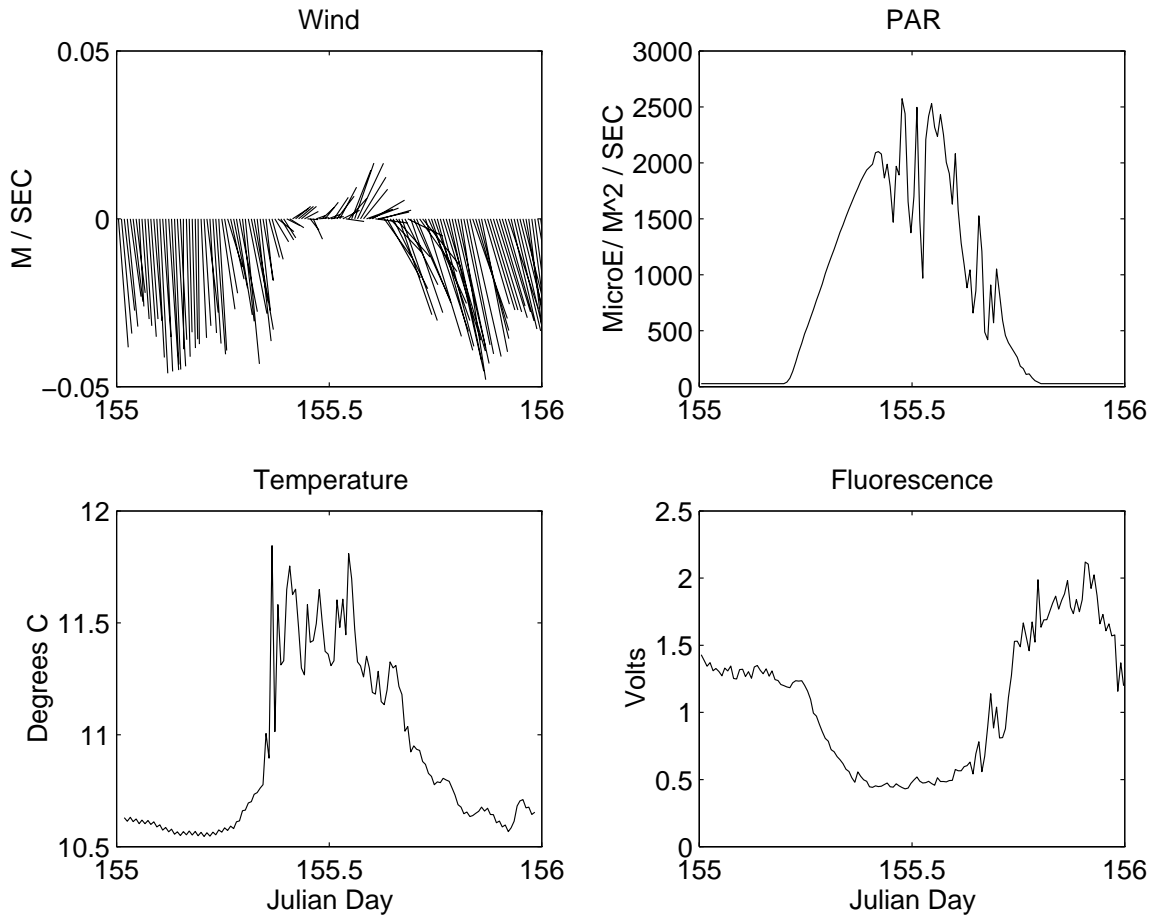


Figure 4. Julian Day 155, 1994, was plotted separately to illustrate the typical daily profile of the four variables temperature, fluorescence, PAR and wind.

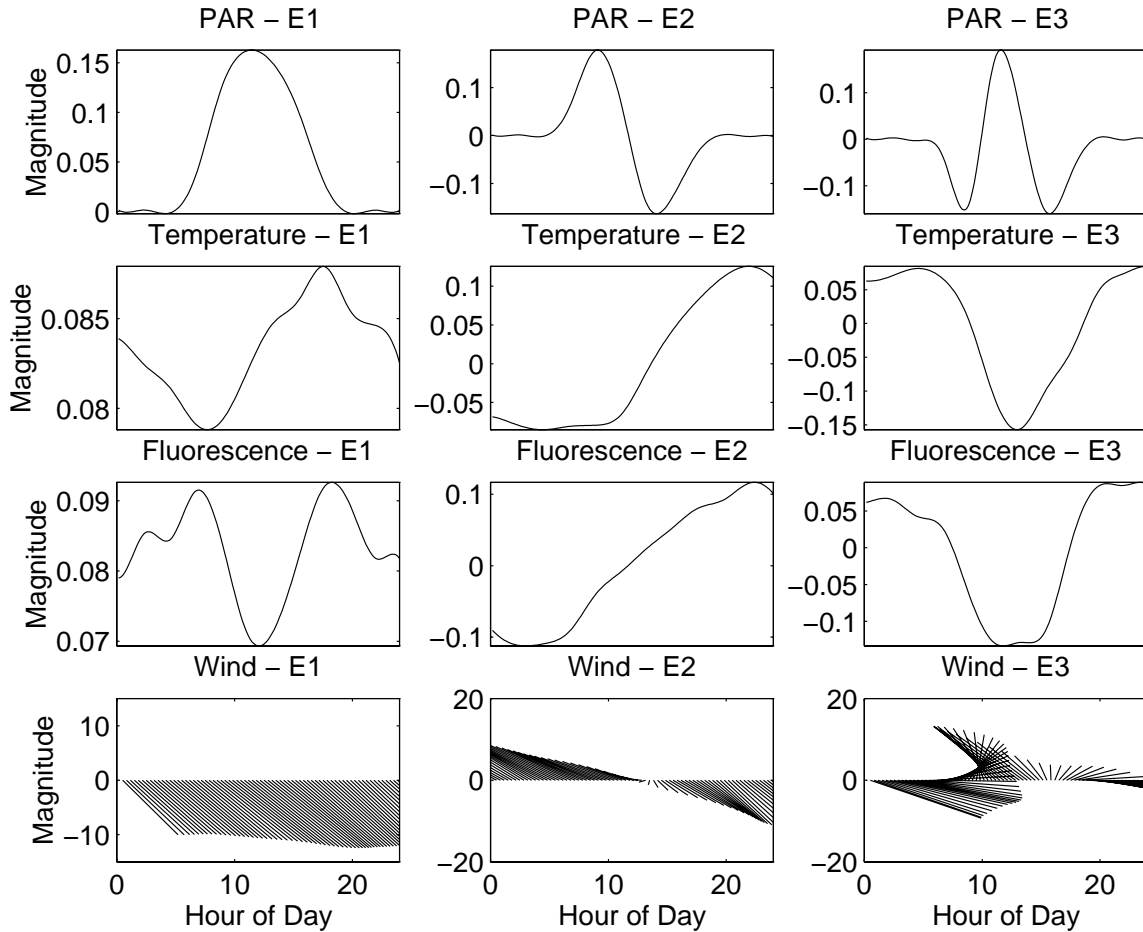


Figure 5. The first three eigenfunctions from the PCA analyses of PAR, temperature, fluorescence and wind. E1- first eigenfunction, E2 - second eigenfunction, E-3 third eigenfunction. The x-axis represents time during a 24-hour day. The y-axis is the magnitude of the eigenfunction, and is the deviation over the mean for that variable. For wind, every other vector was plotted to increase clarity for viewing.

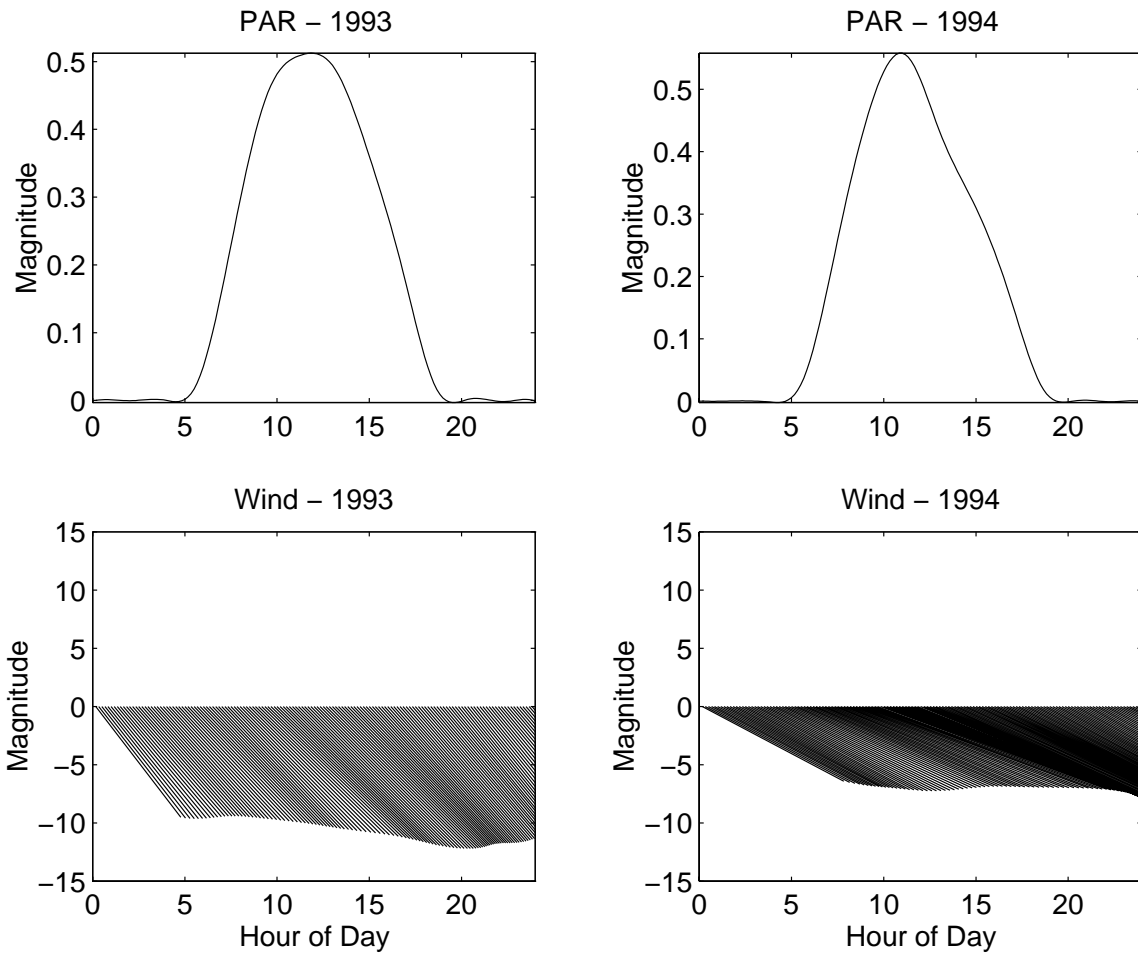


Figure 6. Eigenfunctions from the PCC analysis of PAR and wind in 1993 and 1994.

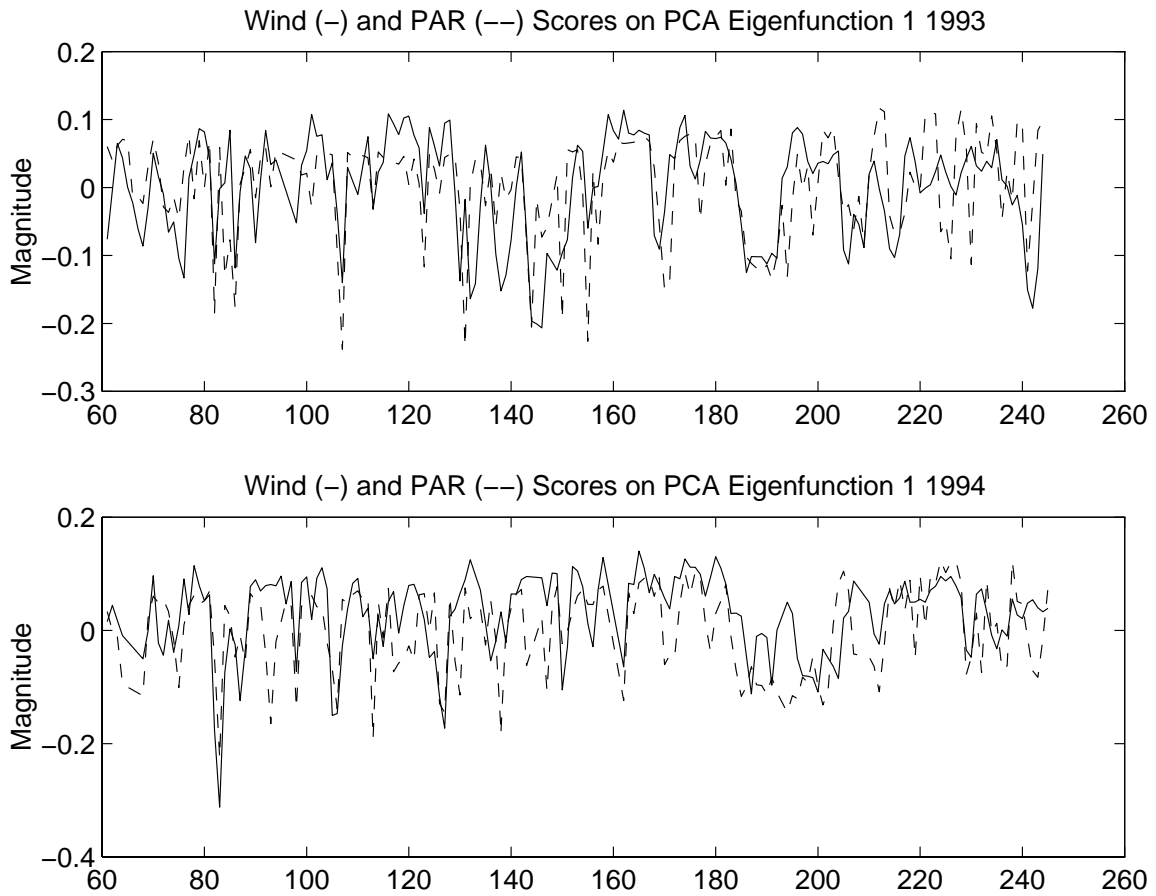


Figure 7. Time series of the scores from the PCC analysis of PAR and wind in 1993 and 1994.

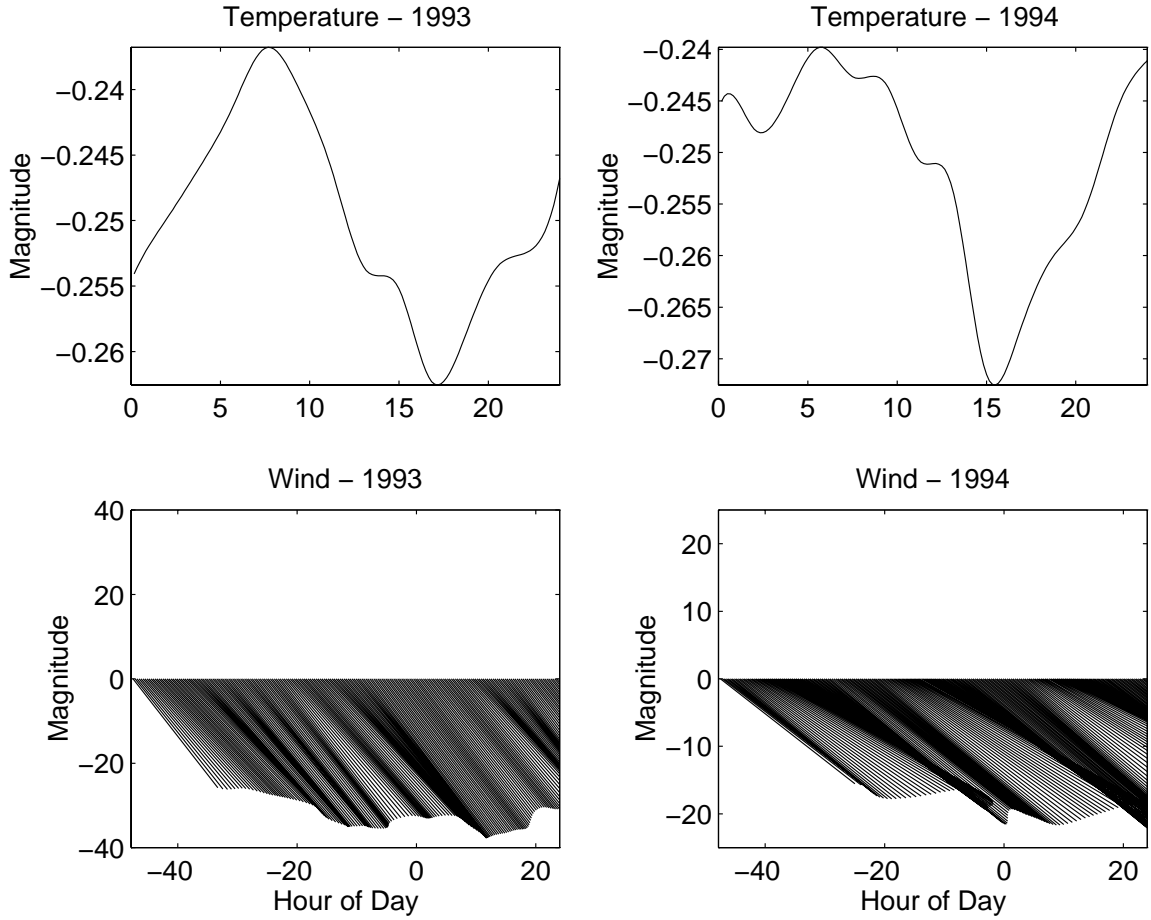


Figure 8. Eigenfunctions from the PCC analysis of temperature and wind in 1993 and 1994. The relationship between temperature on a given day with wind on that day and 2 days previous was examined. The x-axes for the wind eigenfunctions are negative to reflect wind events occurring in the two days prior to the temperature events. For wind, every other vector was plotted to increase clarity for viewing.

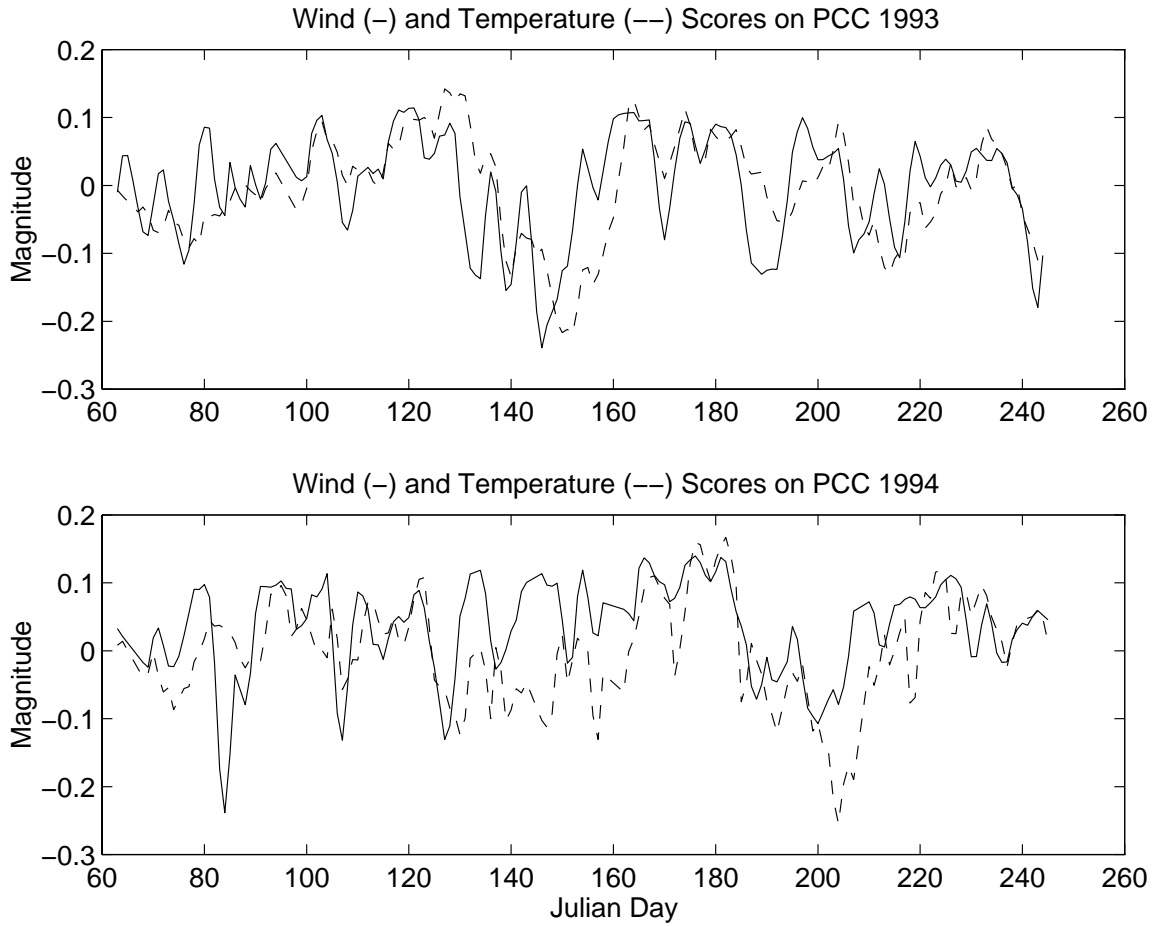


Figure 9. Time series of the scores from the PCC analysis of temperature and wind in 1993 and 1994.

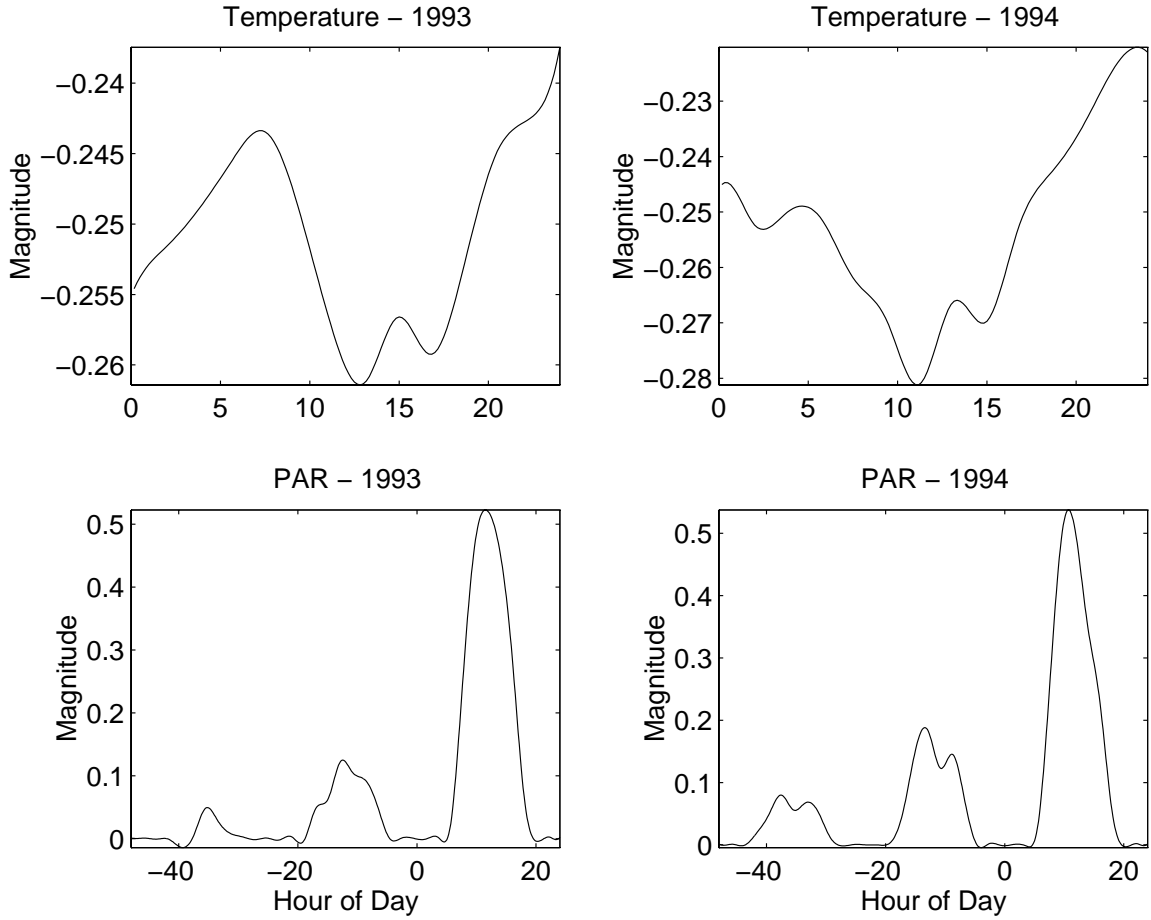


Figure 10. Eigenfunctions from the PCC analysis of temperature and PAR in 1993 and 1994. The relationship between temperature on a given day with PAR on that day and 2 days previous was examined. The x-axes for the PAR eigenfunctions are negative to reflect PAR events occurring in the two days prior to the temperature events.

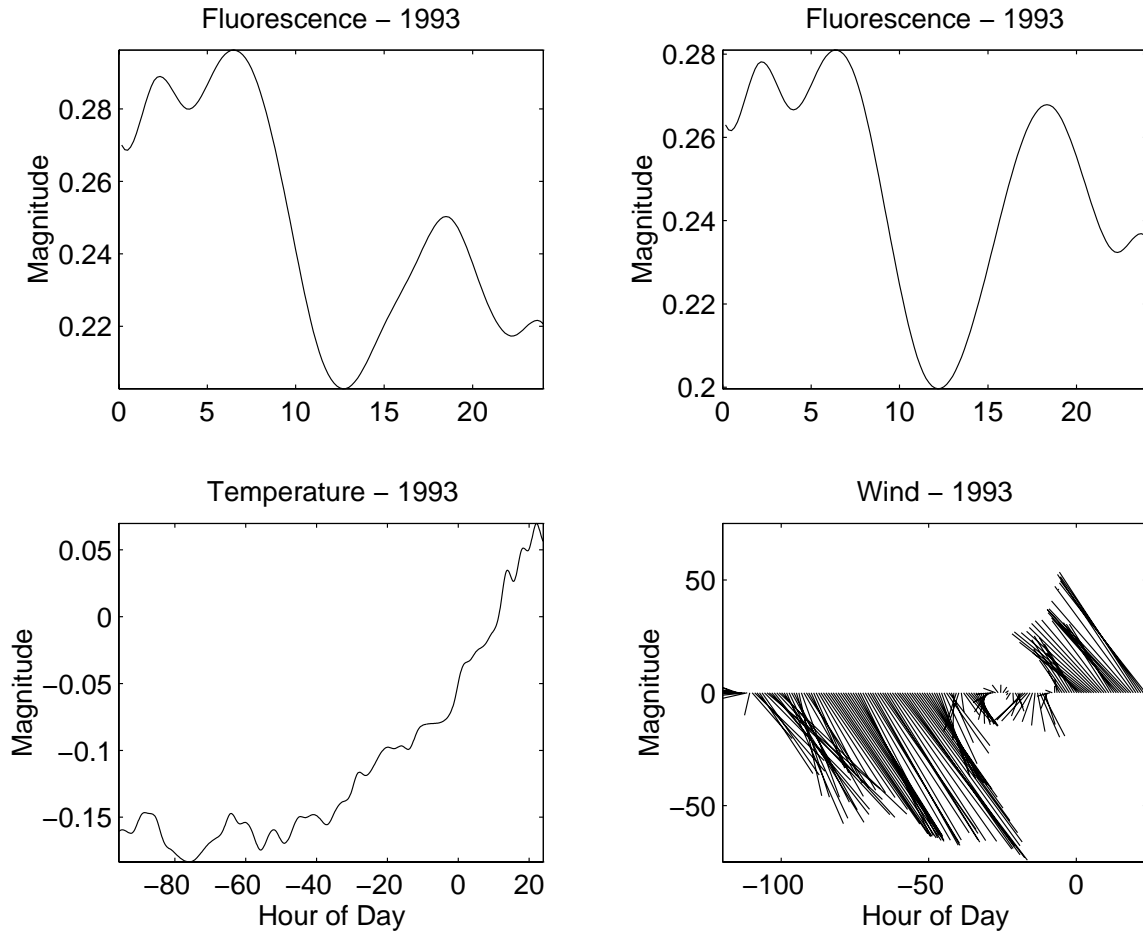


Figure 11. Eigenfunctions from the PCC analysis of fluorescence and temperature, and fluorescence and wind in 1993. The relationship between fluorescence on a given day and temperature on that day and four days previous was examined. The x-axis for temperature is negative to reflect temperature events occurring the four days prior to fluorescence events. In examining the relationship between fluorescence and wind, events in fluorescence on a given day were compared with wind events on that day and five days previously. The x-axis for wind is negative to reflect wind events occurring the five days prior to fluorescence events. For wind, every 5<sup>th</sup> vector is plotted to increase clarity for viewing.